ACS APPLIED MATERIALS & INTERFACES

Research Article

Cite This: ACS Appl. Mater. Interfaces 2019, 11, 16922−16933

www.acsami.org

Fabrication and Characterization of Layer-by-Layer Composite Nanoparticles Based on Zein and Hyaluronic Acid for Codelivery of Curcumin and Quercetagetin

Shuai Chen,[†] Yahong Han,[†] Jingyang Huang,[†] Lei Dai,[†] Juan Du,[‡] David Julian McClements,[§] Like Mao,[†] Jinfang Liu,[†] and Yanxiang Gao*[,†]

[†]Beijing Key Laboratory of Functional Food from Plant Resources, College of Food Science & Nutritional Engineering, China Agricultural University, Beijing 100083, China

[‡]Henan Key Laboratory of Cold Chain Food Quality and Safety Control, Zhengzhou University of Light Industry, Zhengzhou 450001, China

[§]Department of Food Science, University of Massachusetts Amherst, Amherst, Massachusetts 01003, United States

Supporting Information

ABSTRACT: The utilization of layer-by-layer composite nanoparticles fabricated from zein and hyaluronic acid (HA) for the codelivery of curcumin and quercetagetin was investigated. A combination of hydrophobic effects and hydrogen bonding was responsible for the interaction of zein with both curcumin and quercetagetin inside the nanoparticles. Electrostatic attraction and hydrogen bonding were mainly responsible for the layer-by-layer deposition of hyaluronic acid on the surfaces of the nanoparticles. The secondary structure of zein was altered by the presence of the two nutraceuticals and HA. The optimized nanoparticle formulation contained relatively small particles (d = 231.2 nm) that were anionic (ζ = −30.5 mV). The entrapment efficiency and loading capacity were 69.8 and 2.5% for curcumin and 90.3 and 3.5% for quercetagetin, respectively. Interestingly, the morphology of the nanoparticles depended on their composition. In particular, they changed from coated nanoparticles to nanoparticle-filled microgels as the level of HA increased. The nanoparticles were effective at reducing light and thermal degradation of the two encapsulated nutraceuticals and remained physically stable throughout 6 months of long-term storage. In addition, the nanoparticles were shown to slowly release the nutraceuticals under simulated gastrointestinal tract conditions, which may help improve their oral bioavailability. In summary, we have shown that layer-by-layer composite nanoparticles based on zein and HA are an effective codelivery system for two bioactive compounds.

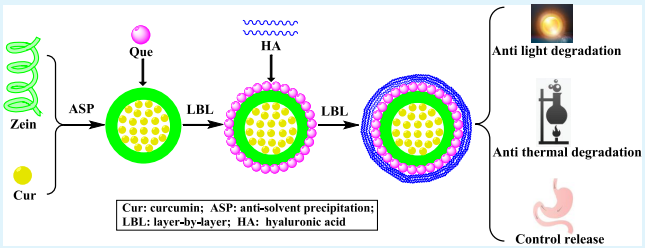

KEYWORDS: *layer-by-layer stepwise deposition, composite nanoparticles, zein, hyaluronic acid, curcumin, quercetagetin*

1. INTRODUCTION

Layer-by-layer (L-B-L) assembly is a promising technology for the development of structured delivery systems to encapsulate, protect, and release bioactive compounds. Positively and negatively charged biopolymers can be sequentially deposited around colloidal particle templates to modulate their interfacial properties, such as thickness, charge, rheology, and permeability, as well as to endow the characteristics of organizational modularity, diversity, and heterogeneity of composition to the delivery system.[1] For most applications, layer-by-layer assembly is driven by electrostatic attraction between oppositely charged biopolymers, but hydrophobic interactions, hydrogen bonding, and specific recognition can also be used.[2] Bioactive compounds with different polarities can be encapsulated within different locations in structured delivery vehicles. For instance, hydrophobic bioactives can be located within the hydrophobic core of lipid or protein nanoparticles, whereas more hydrophilic bioactives can be located in the hydrophilic multilayer shell coating them. The layer-by-layer deposition method allows structured delivery vehicles with novel encapsulation and release properties to be developed.[3,4] For example, poly-L-lactic/glycolic acid particles can be coated by polyallylamine hydrochloride/poly(styrenesulfonate) or poly-L-lysine hydrobromide/dextran sulfate layers using the L-B-L technique, which delays the release of encapsulated bioactive compounds and extends their release time under physiological conditions.[5] Pluronic nanoparticles have been embedded within liposome vesicles to form layer-by-layer structures, which enhanced the permeation and retention time of an anticancer drug (docetaxel) in tumor-bearing mice.[2] The surfaces of bovine serum albumin nanoparticles have been modified with hyaluronic acid (HA) using the L-B-L technique

Received: February 9, 2019
Accepted: April 15, 2019
Published: April 15, 2019

Downloaded via CHINA AGRICULTURAL UNIV on February 3, 2023 at 02:21:24 (UTC).
See https://pubs.acs.org/sharingguidelines for options on how to legitimately share published articles.

© 2019 American Chemical Society

DOI: 10.1021/acsami.9b02529
ACS Appl. Mater. Interfaces 2019, 11, 16922−16933

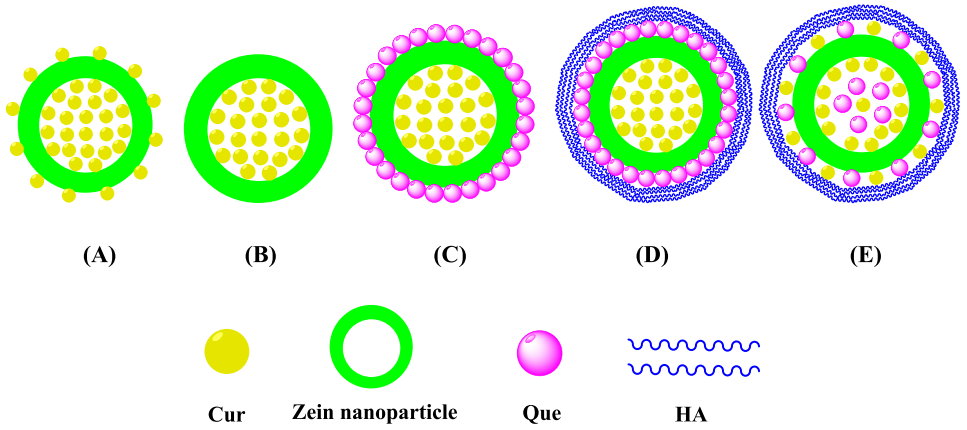

Figure 1. (A) Cur−zein (ASP) nanoparticle (before washing), (B) Cur−zein nanoparticle (after washing), (C) Cur−zein−Que nanoparticle, (D) Cur−zein−Que−HA nanoparticle, and (E) Cur−Que−zein−HA nanoparticle.

to deliver anticancer agents (doxorubicin) into cancer cells in a customized amount and a targeted manner.[3]

Proteins and polysaccharides are usually utilized as the host material for layer-by-layer assembly in food and drug products due to their biodegradable, biocompatible, and nontoxic properties. Zein is a hydrophobic protein that is commonly used to assemble structured delivery systems in food and industrial applications, for example, biodegradable films,[6] coatings,[7] nanofibers,[8] inks,[9] and colloidal delivery vehicles.[10] In particular, zein has been widely used to create protein nanoparticles that are able to incorporate and deliver nonpolar bioactive molecules, such as nutraceuticals, vitamins, and supplements. However, the widespread application of zein nanoparticles is often limited by their poor physical stability, such as their tendency to aggregate and precipitate when exposed to acid, base, metal ions, and high temperatures. Previous studies have shown that their stability can be improved by coating them with polysaccharides.[10] Hyaluronic acid (HA) is a polysaccharide made up of multiple disaccharide units of *N*-acetyl-D-glucosamine and D-glucuronic acid.[11] The incorporation of HA into colloidal delivery systems has previously been shown to improve their drug retention and delivery profiles.[3,12] HA may also be a useful building block for fabricating delivery vehicles for drugs and nutraceuticals.[13] Moreover, it also has many useful biological activities, such as its ability to modulate inflammation, aging, angiogenesis, and embryonic development.[14,15]

Curcumin (Cur) is a natural polyphenol with many physiological functions. Due to its wide applications in the prevention and treatment of many chronic diseases, such as Parkinson's disease, Alzheimer's disease, and multiple sclerosis, curcumin is regarded as a "next-generation multipurpose drug".[16,17] Quercetagetin (Que) is also a bioactive compound found in some natural plants. It could be used as an antioxidant, antimicrobial, and anti-inflammatory agent,[18] and it reduces the risk of cancer, cardiovascular disease, and other chronic diseases.[19,20] However, both curcumin and quercetagetin are chemically unstable, have low water solubility, and poor bioavailability, which greatly limit their applications in the food, supplement, and drug industries. For this reason, researchers are examining the application of various types of nanoparticles to overcome these problems. This is often challenging because differences in the molecular structure and polarity of these two nutraceuticals makes it difficult to encapsulate them in a single nanoparticle. In previous studies, no single delivery system has been designed to deliver both curcumin and quercetagetin.

Recently, the development of codelivery systems has become an area of active research because of their potential to deliver several beneficial bioactive agents simultaneously. This approach has many advantages, such as the ability to formulate the proportion and dosage of different bioactive agents, control the release time and release rate of each drug independently, and achieve synergistic effects.[21,22] Therefore, a codelivery system for curcumin and quercetagetin was developed in this study. These systems were made up of a hydrophobic protein core (zein) and a hydrophilic polysaccharide shell (HA) using an L-B-L electrostatic deposition method.[23] Curcumin, which is a highly hydrophobic molecule,[24] was encapsulated within the hydrophobic core of the zein nanoparticles, whereas quercetagetin, which is more polar, was adsorbed to their hydrophilic surfaces. The present work might contribute to the development of more effective codelivery systems for multiple bioactive agents, which may be useful for benefiting from synergistic interactions between bioactives.

2. MATERIALS AND METHODS

2.1. Materials. Zein (95%) was obtained from Sigma-Aldrich. Hyaluronic acid (HA, 99%) was provided by the Xi'an Baichuan Group (Xi'an, China). Quercetagetin (Que, 95%) was extracted from *Tagetes erecta* using the procedure described in our previous report.[18] Curcumin (Cur, 98%) was provided by the China National Medicine Group (Shanghai, China). Ethanol (99.9%) was purchased from the Beijing Chemical Group (Beijing, China).

2.2. Fabrication of Layer-by-Layer Composite Nanoparticles. L-B-L assembly methods were used to fabricate the structured nanoparticles developed in this study. First, zein (2.4 g) and curcumin (120.0 mg) were dissolved in a 240.0 mL aqueous ethanol (70%, v/v) solution. The resulting mixture was then injected (20.0 mL/min) into 720.0 mL of distilled water and stirred for 20 min at 600 rpm, which led to the formation of curcumin-loaded zein nanoparticles due to antisolvent precipitation (ASP). Ethanol was removed at 40 °C under −0.1 MPa from the resulting colloidal suspension using a rotary evaporator. The samples prepared using the ASP method are referred to as Cur−zein (5:100, ASP) nanoparticles (Figure 1A).

Second, a mixture (v/v, 1:1) of *n*-hexane and ethyl acetate was used to wash the residual curcumin from the surfaces of the Cur−zein (5:100, ASP) nanoparticles. The organic phase and aqueous phase were mixed together in a closed separation funnel and then shaken for a short time. The mixture was then left to stand for 10 min. The lower aqueous phase was then poured into a flask and any residual organic reagents within it were removed using a rotary evaporator (40 °C,

DOI: 10.1021/acsami.9b02529
ACS Appl. Mater. Interfaces 2019, 11, 16922−16933

−0.1 MPa). The effect of the number of washing steps on the retention of the curcumin by the particles was studied, and it was found that one wash was optimum. The washed sample is referred to as Cur−zein (5:100) nanoparticles (Figure 1B).

Third, different quantities of quercetagetin (10.0, 20.0, 30.0, and 40.0 mg) were dissolved in aqueous ethanol solutions (70%, v/v, 10.0 mL). The resulting mixtures were then injected into four equal volumes (66.0 mL) of Cur−zein (5:100) nanoparticle dispersions at 20.0 mL/min, respectively. The samples were stirred (600 rpm) for 20 min to allow quercetagetin to adsorb as much as possible onto the surfaces of the Cur−zein (5:100) nanoparticles. The resulting samples were referred to as Cur−zein−Que (5:100:5, 5:100:10, 5:100:15, and 5:100:20) nanoparticles (Figure 1C). These nanoparticles were injected (20.0 mL/min) into a HA (40.0 mg) aqueous solution with stirring at 600 rpm for 20 min. The resulting samples were referred to as Cur−zein−Que−HA (5:100:5:20, 5:100:10:20, 5:100:15:20, and 5:100:20:20) nanoparticles (Figure 1D).

Fourth, Cur−zein−Que (5:100:5) nanoparticle dispersions were injected into an equal volume of HA (20.0, 30.0, 40.0, 50.0, and 60.0 mg) aqueous solution at 20.0 mL/min with continuous stirring at 600 rpm for 20 min. The resulting samples were referred to as Cur−zein−Que−HA (5:100:5:10, 5:100:5:15, 5:100:5:20, 5:100:5:25, and 5:100:5:30) nanoparticles (Figure 1D).

Finally, Cur−Que−zein−HA (5:5:100:20) nanoparticles (Figure 1E) were prepared as controls. In this case, the two nutraceuticals were co-encapsulated inside the zein nanoparticles, rather than having the curcumin inside and the quercetagetin outside. This was achieved by dissolving zein (200.0 mg), curcumin (10.0 mg), and quercetagetin (10.0 mg) in 70% (v/v) aqueous ethanol solution (20.0 mL). Thereafter, 20 mL of this mixed solution was injected into (20.0 mL/min) 60.0 mL of distilled water and then stirred at 600 rpm (20 min). Finally, ethanol was removed at 40 °C under −0.1 MPa by a rotary evaporator. The insoluble substances, such as free curcumin and quercetagetin, were removed by centrifugation (3000 rpm, 10 min). The nanoparticle dispersion was then injected into HA aqueous solution (contain HA 40.0 mg) at 20.0 mL/min to form Cur−Que−zein−HA (5:5:100:20) nanoparticles (Figure 1E).

2.3. Characterization of Layer-by-Layer Composite Nanoparticles. *2.3.1. Particle Characteristics.* Particle size and ζ-potential of the nanoparticles were measured by a combined particle electrophoresis/dynamic light-scattering instrument according to our previous report.[25] The turbidity was determined using a laboratory turbidimeter (HACH 2100N, Loveland) according to our previous report.[26]

The curcumin content of the nanoparticles was measured according to a method described previously.[27] Briefly, the curcumin was extracted from the nanoparticle dispersion using an 80% (v/v) aqueous ethanol solution with an ultrasound-assisted method. The curcumin content in the aqueous ethanol solutions was then analyzed by a spectrophotometer (UV-1800, Japan) at 426 nm. The entrapment efficiency (EE) and loading capacity (LC) of the curcumin were then calculated using the following expressions[27]

$$\mathrm{EE} = \frac{\text{encapsulated Cur}}{\text{total Cur}} \times 100\% \quad (1)$$

$$\mathrm{LC} = \frac{\text{encapsulated Cur}}{\text{total mass of nanoparticles}} \times 100\% \quad (2)$$

The quercetagetin content of the nanoparticles was measured according to a previous method.[25] Briefly, the samples were centrifuged at 15 000 g for 30 min to separate the particles. The supernatant was then removed and diluted with 70% (v/v) aqueous ethanol solution. The quercetagetin content in the aqueous ethanol solution was then analyzed by a spectrophotometer operating at 360 nm. The EE and LC of the quercetagetin were then calculated using the following expressions[25]

$$\mathrm{EE} = \frac{\text{total Que} - \text{free Que}}{\text{total Que}} \times 100\% \quad (3)$$

$$\mathrm{LC} = \frac{\text{total Que} - \text{free Que}}{\text{total mass of nanoparticles}} \times 100\% \quad (4)$$

2.3.2. Fourier Transform Infrared (FTIR), Circular Dichroism, Fluorescence Spectra, and Field Emission Scanning Electron Microscopy (FE-SEM). The FTIR spectra of the nanoparticles were measured in the wavenumber range from 400 to 4000 cm^{-1} according to a previous report.[25] Sixteen scans were performed for each measurement at a resolution of 4 cm^{-1}. The operating parameters used in the circular dichroism instrument were set as follows: 190−260 nm far-UV wavelength, 2.0 nm band width, 100 nm/min recorded speed, 0.1 cm path length, 0.2 nm resolution, and 20 accumulations. The secondary structure fractions of the protein in the nanoparticles were calculated according to a CD website (http://dichroweb.cryst.bbk.ac.uk).[28] It should be noted that zein is actually a mixture of proteins (19 and 22 kDa) and so the calculated secondary structure will only be an average for the whole system.

The operating parameters used for the fluorescence spectra measurements were as follows: the nanoparticle concentration in dispersions was 0.25 mg/mL; the excitation wavelength was 280 nm; the scanning rate was 100 nm/min; the spectra range was 290−450 nm; and emission and excitation slit widths were 10 nm.[27]

Microtopography of the lyophilized L-B-L nanoparticles was preformed using a field-emission scanning electron microscope (SU8010, Hitachi). The dried samples were sputter-coated with a gold layer before observation to avoid charging under the electron beam.[27]

2.4. Simulated Gastrointestinal Digestion. The potential gastrointestinal fate of the nanoparticle dispersions was tested according to a method described previously.[29] First, 30 mL of L-B-L nanoparticle dispersions were mixed with 30 mL of simulated gastric fluid (SGF: includes 3.2 mg/mL pepsin and 2.0 mg/mL NaCl) in a glass flask. The pH of the mixtures was adjusted to 1.2 using hydrochloric acid (1.0 M), and then the system was incubated at 37.0 °C in a water bath shaker. Samples were collected at 30 and 60 min. The gastric digestion mixtures were then adjusted to pH 7.5 using sodium hydroxide (1.0 M). The mixtures (30 mL) were added into 30 mL of simulated intestinal fluid (SIF: includes 12.0 mg/mL bile salts, 2.0 mg/mL pancreatin, 6.8 mg/mL KH_2PO4, and 8.8 mg/mL NaCl). The mixtures were incubated at 37 °C in a water bath shaker, and samples were collected at 30, 60, 90, and 120 min. The curcumin and quercetagetin contents in the nanoparticles collected at different digestion stages were measured using the method described in Section 2.3.1.

2.5. Nutraceutical Stability. *2.5.1. Thermal Degradation Kinetics.* The thermal degradation kinetics of curcumin and quercetagetin in the nanoparticles were estimated according to a method reported previously.[27] Briefly, the nanoparticle dispersions were placed in transparent sample bottles and then incubated at 80 °C for 2, 4, 6, 8, and 10 h in a thermostatic water bath. After the test, the contents of curcumin and quercetagetin were determined by the methods described previously.

2.5.2. Light Degradation Kinetics. The light degradation kinetics of curcumin and quercetagetin in the nanoparticles were estimated referring to a method reported previously.[10] For these experiments, the light intensity and temperature were set at 0.35 W/m^2 and 35°C, respectively, and samples were collected at 20, 40, 60, 80, 120, 240, and 360 min. The curcumin and quercetagetin contents of the samples were determined using the methods described earlier. The degradation rate constant (k) and half-life ($t_{1/2}$) values were calculated using the following expressions[30]

$$\ln(C/C_0) = -kt \quad (5)$$

$$t_{1/2} = \frac{\ln 2}{k} \quad (6)$$

Here, C_0 and C represent the concentrations at time 0 and t, respectively.

2.5.3. Long-Term Storage Stability. Nanoparticle dispersions were stored under refrigerated conditions (4 °C) for an extended time, and

DOI: 10.1021/acsami.9b02529
ACS Appl. Mater. Interfaces 2019, 11, 16922−16933

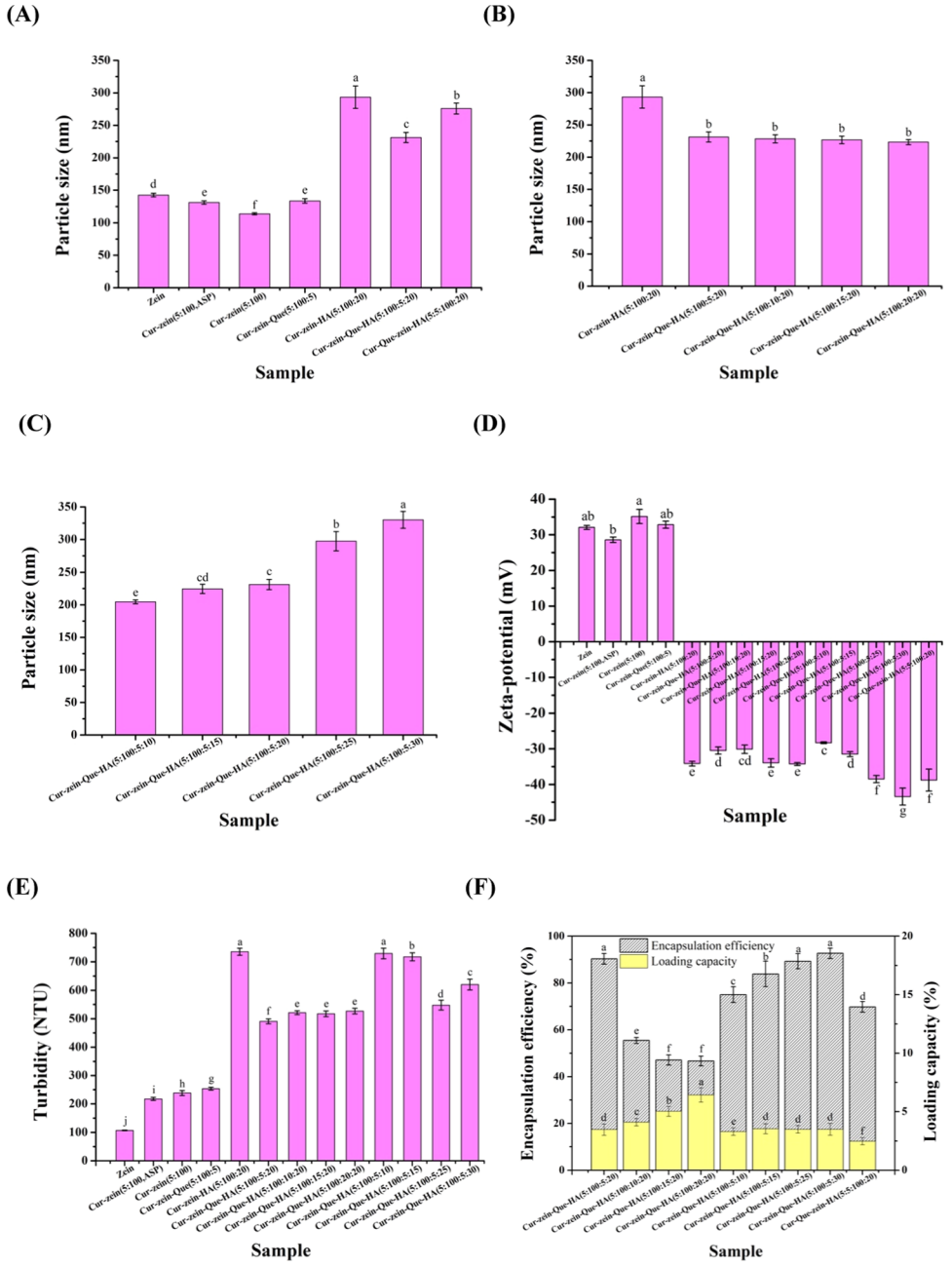

Figure 2. Particle size (A–C), ζ-potential (D), and turbidity (E) of Cur–zein–Que–HA L-B-L nanoparticles; entrapment efficiency and loading capacity of quercetagetin in Cur–zein–Que–HA L-B-L nanoparticles (F).

changes in their properties were measured. The particle diameter and ζ-potential were analyzed using the methods described earlier. The retention rates (%) of the two nutraceuticals after long-term storage were estimated using the following equations[10]

$$\text{retention rate of Que}(\%) = \frac{\text{the amount of Que after storge}}{\text{the initial amount of Que}} \times 100\% \quad (7)$$

$$\text{retention rate of Cur}(\%) = \frac{\text{the amount of Cur after storge}}{\text{the initial amount of Cur}} \times 100\% \quad (8)$$

2.6. Statistical Analysis. All experiments were performed three times, and the mean and standard deviation were calculated from these data. Data were analyzed using analysis of variance, and $p < 0.05$ was identified as being significantly different.

3. RESULTS AND DISCUSSION

3.1. Particle Size, ζ-Potential, and Turbidity. The mean particle diameter of the L-B-L nanoparticles is shown in Figure 2A–C. Pure zein nanoparticles had a mean diameter of 142.7 nm, which was slightly higher than that observed for the Cur–zein (5:100, ASP) nanoparticles (131.3 nm). This effect may have occurred because polyphenols bound to the hydrophobic zein molecules and altered nanoparticle formation during antisolvent precipitation.[31] After removing the curcumin adsorbed to the nanoparticle surfaces using organic solvents, the size of the Cur–zein nanoparticles decreased to around 114.0 nm. When quercetagetin was adsorbed to the outer

DOI: 10.1021/acsami.9b02529
ACS Appl. Mater. Interfaces 2019, 11, 16922–16933

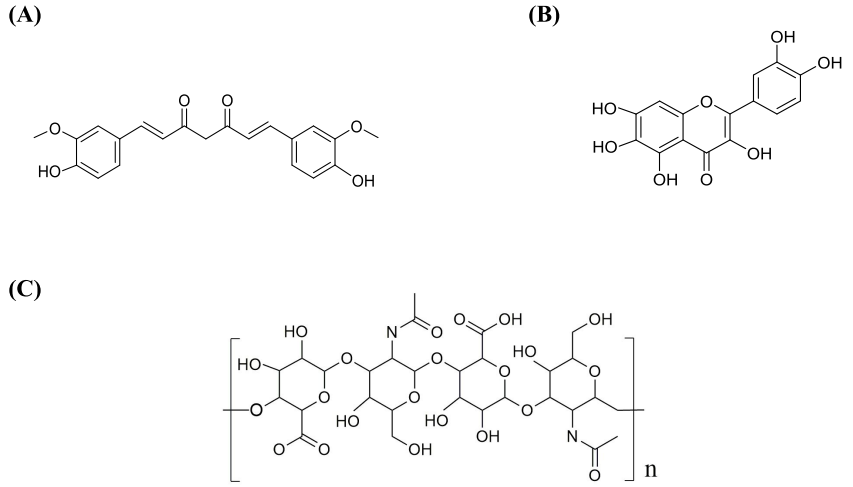

Figure 3. Molecular structures of curcumin (A), quercetagetin (B), and hyaluronic acid (C).

surfaces of the Cur−zein nanoparticles, the mean diameter of the Cur−zein−Que nanoparticles increased to 133.7 nm. Similarly, when HA adsorbed on the outer layer of the Cur−zein−Que nanoparticles, the mean particle diameter increased further to 231.2 nm. This phenomenon agreed with our previous research, which showed that the incorporation of polysaccharides can greatly increase the size of polyphenol−protein nanoparticles.[25]

Interestingly, the size of the Cur−zein−Que−HA (5:100:5:20) nanoparticles was smaller than that of the Cur−zein−HA (5:100:20) nanoparticles (Figure 2B). Presumably, the quercetagetin interacted with the HA molecules in the outer layer of the nanoparticles, thereby causing them to pack more closely. In our previous report, we found that the dimensions of zein−propylene glycol alginate (PGA) nanoparticles also decreased when they were combined with quercetagetin.[25] However, there was no obvious difference among the sizes of Cur−zein−Que−HA (5:100:5:20, 5:100:10:20, 5:100:15:20, and 5:100:20:20) nanoparticles with different levels of quercetagetin. It is possible that the quercetagetin in the outer layer of the Cur−zein−Que nanoparticles was close to its saturation level when the mass ratio of Cur−zein−Que−HA was 5:100:5:20. Consequently, any additional quercetagetin could not adsorb to the Cur−zein−Que nanoparticles. Instead, it was insoluble and formed visible sediments at the bottom of the sample bottles. The effect of the HA level on the mean size of the nanoparticles is illustrated in Figure 2C. The nanoparticles gradually became larger as the HA level was increased. A similar trend was reported for zein−chitosan nanoparticles, where the particle size increased as the chitosan level was raised.[32]

The ζ-potential values of the nanoparticles are shown in Figure 2D. Zein, Cur−zein (5:100, ASP), Cur−zein (5:100), and Cur−zein−Que (5:100:5) nanoparticles were positively charged, which can be attributed to the pH of the solution being below the isoelectric point of zein. However, all of the nanoparticles became strongly negatively charged when they were coated with HA, which can be attributed to the high negative charge (−49.3 mV) associated with this polymer. This result suggests that electrostatic attraction was the main driving force for the adsorption of HA on to the outer layer of the Cur−zein−Que (5:100:5) nanoparticles. A similar phenomenon has also been reported for lactoferrin−pectin nanoparticles[33] and for lactoferrin−high methoxyl pectin nanoparticles.[34] At a constant HA level, the ζ-potential values for the Cur−zein−Que−HA (5:100:5:20, 5:100:10:20, 5:100:15:20, and 5:100:20:20) nanoparticles were all similar, suggesting that quercetagetin did not have an obvious impact on the net charge of the nanoparticles. With increasing HA concentration, the ζ-potential values of the Cur−zein−Que−HA L-B-L nanoparticles (5:100:5:10 to 5:100:5:30) decreased from −28.3 to −43.8 mV.

As shown in Figure 2E, the turbidity (217.3 NTU) of the Cur−zein (5:100, ASP) nanoparticles was appreciably higher than the turbidity (106.8 NTU) of the zein nanoparticles. This phenomenon may have been because the curcumin absorbed some of the light, thereby leading to a reduction in the amount detected. In the presence of HA, the turbidity of the nanoparticles increased significantly ($p < 0.05$), which may have been because the increase in particle size led to more light scattering.

3.2. Entrapment Efficiency and Loading Capacity. As shown in Figure 2F, the entrapment efficiency of quercetagetin in the Cur−zein−Que−HA (5:100:5:20) nanoparticles was around 90.3%. However, this value reduced significantly ($p < 0.05$) as the total level of quercetagetin in the system increased to 55.4, 47.1, and 46.7% for 5:100:10:20, 5:100:15:20, and 5:100:20:20 Cur−zein−Que−HA nanoparticles, respectively. This result suggests that quercetagetin adsorbed to the surfaces of the Cur−zein−Que−HA nanoparticles until saturation occurred. After this point, any additional quercetagetin aggregated and sedimented at the bottom of the samples. The hypothesis was supported by the fact that increasing the quercetagetin level had no significant impact on the size, ζ-potential, or turbidity of the Cur−zein−Que−HA nanoparticles (5:100:10:20, 5:100:15:20, and 5:100:20:20).

When the level of quercetagetin was held constant and the concentration of HA was increased, the entrapment efficiency of quercetagetin gradually increased from 75.0% (Cur−zein−Que−HA, 5:100:5:10) to 92.7% (Cur−zein−Que−HA, 5:100:5:30). This result indicated that the presence of HA greatly enhanced the entrapment efficiency of quercetagetin in the Cur−zein−Que−HA nanoparticles. A similar finding has been reported for quercetagetin-loaded zein nanoparticles combined with PGA.[35]

For quercetagetin, the EE (90.3%) and LC (3.5%) values for the Cur−zein−Que−HA (5:100:5:20) nanoparticles were appreciably higher than the EE (69.8%) and LC (2.5%) values

DOI: 10.1021/acsami.9b02529
ACS Appl. Mater. Interfaces 2019, 11, 16922−16933

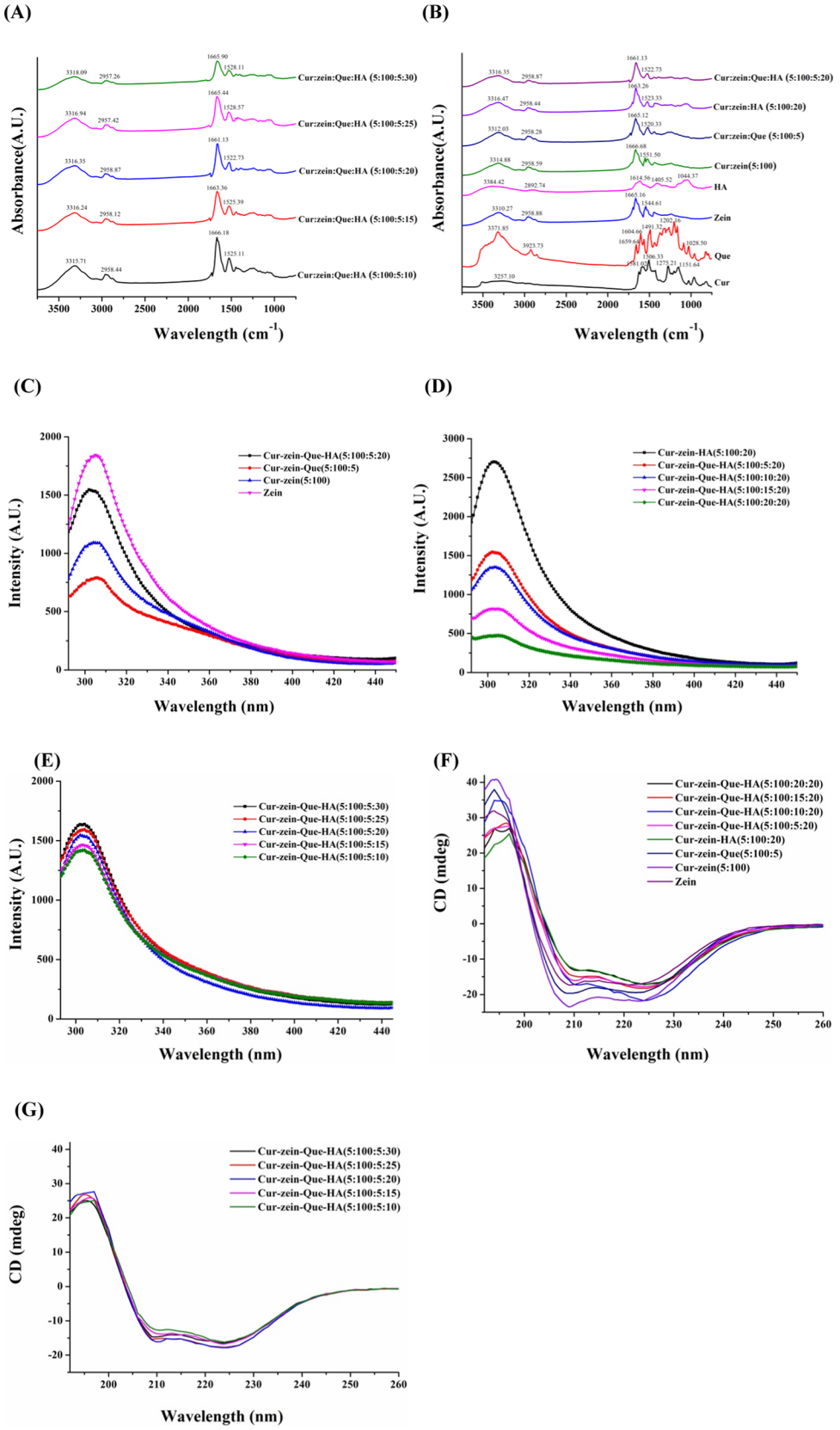

Figure 4. FTIR spectra (A, B), fluorescence spectra (C–E), and circular dichroism spectra (F, G) of Cur–zein–Que–HA nanoparticles.

for the Cur–zein–Que–HA (5:5:100:20) nanoparticles. Conversely, for curcumin, the Cur–zein–Que–HA (5:100:5:20) nanoparticles (EE 51.8% and LC 2.0%) exhibited better EE and LC than the Cur–Que–zein–HA (5:5:100:20) nanoparticles (EE 31.3% and LC 1.2%). The result was attributed to the fact that that both quercetagetin and curcumin competed for hydrogen bonding and for hydrophobic binding sites on the zein molecules during the

DOI: 10.1021/acsami.9b02529
ACS Appl. Mater. Interfaces 2019, 11, 16922–16933

preparation of the Cur−Que−zein−HA (5:5:100:20) nanoparticles. However, in the case of the Cur−zein−Que−HA (5:100:5:20) nanoparticles, there was no competition between the two nutraceuticals because they were in different locations (curcumin inside and quercetagetin outside).

The layer-by-layer structure of the nanoparticles was designed based on the known molecular characteristics of the different components. As shown in Figure 3A−C, there exist 2, 6, and 10 hydroxyl groups in curcumin, quercetagetin, and hyaluronic acid units, respectively. In general, the more the number of hydroxyl groups, the more polar the molecule;[36] hence, the polarity of curcumin is lower than that of quercetagetin. The more nonpolar curcumin molecules were therefore preferentially encapsulated within the hydrophobic cavity of the zein nanoparticles. Conversely, quercetagetin with a higher polarity was absorbed on the hydrophilic outer layer of the zein nanoparticles and coated by a layer of HA. Consequently, both the EE and LC of curcumin and quercetagetin in the Cur−zein−Que−HA L-B-L nanoparticles (5:100:5:20) were relatively high.

3.3. FTIR. FTIR was used to investigate the nature of the molecular interactions occurring inside the nanoparticles (Figure 4A,B). For curcumin, the peak at 3257.10 cm^{-1} was ascribed to the stretching of the −OH groups on the benzene ring, and the peak at 1506.33 cm^{-1} was ascribed to vibrations of the C−C and C−O groups.[37] Moreover, the peak at 1581.02 cm^{-1} represented the stretching vibration of aromatic rings,[38] and the peak at 1275.21 cm^{-1} was attributed to enolic C−O stretching.[39]

The FTIR spectra from 1028.50 to 1659.64 cm^{-1} of quercetagetin were similar to those of curcumin, but the −OH stretching peak (3371.85 cm^{-1}) was higher and stronger than that for curcumin, in agreement with their molecular structures (Figure 3). The peaks observed from 1000 to 1500 cm^{-1} for curcumin and quercetagetin scarcely appeared in the spectra of the Cur−zein−Que−HA nanoparticles, which confirmed that the two nutraceuticals were successfully encapsulated in the nanoparticles.

In the spectrum of native zein, the peaks at 3310.27, 1665.16, and 1544.61 cm^{-1} were ascribed to the −OH stretching,[40] C−O stretching (amide I), and C−N stretching coupled with the N−H bending mode (amide II), respectively.[41] When zein was combined with curcumin, the peak associated with the amide II groups shifted from 1544.61 to 1551.50 cm^{-1}, which suggests that there were some hydrophobic interactions between these two components. The position of the peak associated with the hydroxy groups moved from 3310.27 to 3314.88 cm^{-1}, which suggested that there was hydrogen bonding between curcumin and zein within the nanoparticles. Hydrophobic interactions and hydrogen bonding also played an important role during the formation of the Cur−zein−Que and Cur−zein−Que−HA L-B-L nanoparticles (Figure 4A,B). When the level of HA in the Cur−zein−Que−HA L-B-L nanoparticles was increased, the peaks associated with the amide (I and II) groups altered from 1666.18 and 1525.11 cm^{-1} (Cur−zein−Que−HA, 5:100:5:10) to 1661.13 and 1522.73 cm^{-1} (5:100:5:20). Nevertheless, no obvious change was found for the peak associated with the −OH groups, indicating that hydrogen bonding was considerably weaker than hydrophobic effects. The peaks associated with the −OH and amide (I and II) groups in the spectrum of the Cur−zein−Que−HA L-B-L nanoparticles were altered from 3316.35, 1661.13, and 1522.73 cm^{-1} (5:100:5:20) to 3318.09, 1665.90, and 1528.11 cm^{-1} (5:100:5:30), respectively. This shift suggests that both hydrophobic interaction and hydrogen bonding were important binding forces in this case (Figure 4B). Luo, Teng, and Wang[42] have reported that hydrogen bonding is also an important binding force within the zein−carboxymethyl chitosan−vitamin D_3 composite nanoparticles.

3.4. Fluorescence Spectra. Fluorescence measurements were carried out to acquire more information about the structural changes and intermolecular interactions occurring within the nanoparticles. As shown in Figure 4C, native zein had a fluorescence excitation peak at 280 nm and an emission fluorescence peak at 305 nm, which was attributed to its tyrosine and tryptophan residues.[35,41] The incorporation of curcumin into the zein nanoparticles obviously decreased the intensity of the emission maximum. Furthermore, the adsorption of quercetagetin onto the particles further decreased the fluorescence intensity. These results can be ascribed to the incorporation of polyphenols, which promote fluorescence quenching of zein through molecular interactions such as rearrangement, energy transduction, collisional quenching, and the formation of a ground state complex.[43] Thus, as the quercetagetin level was increased, the fluorescence intensity of the Cur−zein−Que−HA nanoparticles (5:100:5:10 to 5:100:20:20) decreased (Figure 4D). Conversely, when HA was incorporated into the outer layer of the Cur−zein−Que nanoparticles, the fluorescence intensity increased. This phenomenon may have occurred because HA induced a conformational change in the zein molecules, which exposed some of the tryptophan residues originally hidden within their hydrophobic cores.[33] In general, conformational changes of proteins are known to impact the fluorescence intensity of the tryptophan residues.[44] With increasing HA levels, the fluorescence intensity gradually increased in the Cur−zein−Que−HA (5:100:5:10 to 5:100:5:30) nanoparticles (Figure 4E).

3.5. Circular Dichroism Analysis. The circular dichroism spectrum of native zein nanoparticles showed two characteristic troughs at 209 and 223 nm (Figure 4F).[45] The secondary structure of zein was determined from this spectrum (Table S1). After curcumin was incorporated into the zein nanoparticles (Cur: zein, 5:100), the α-helix content decreased from 32.5 to 26.5% and the β-sheet content increased from 17.9 to 22.9%. The adsorption of quercetagetin onto the Cur−zein−Que nanoparticles led to a decrease in the α-helix content and an increase in the β-sheet content. These results were in line with the study of Sun et al.[46] The origin of this effect may be that there was hydrogen bonding (between the amino of zein and the hydroxyl of Cur) and hydrophobic interactions (hydrocarbyl) between curcumin and zein as well as hydrogen bonding between quercetagetin and zein. These driving forces could lead to the unfolding and reorganization of the zein molecules, which would lead to a change in their secondary structure. When Cur−zein−Que nanoparticles were coated with HA, the α-helix content of zein decreased from 23.6% (Cur−zein−Que, 5:100:5) to 19.4% (Cur−zein−Que−HA, 5:100:5:10), whereas the β-sheet content increased from 26.5 to 29.3%. Hydrogen bonding and electrostatic attraction were considered to be the main binding forces among curcumin, zein, quercetagetin, and HA, which was consistent with the FTIR analysis. When the amount of HA in the Cur−zein−Que−HA L-B-L nanoparticles was altered from

DOI: 10.1021/acsami.9b02529
ACS Appl. Mater. Interfaces 2019, 11, 16922−16933

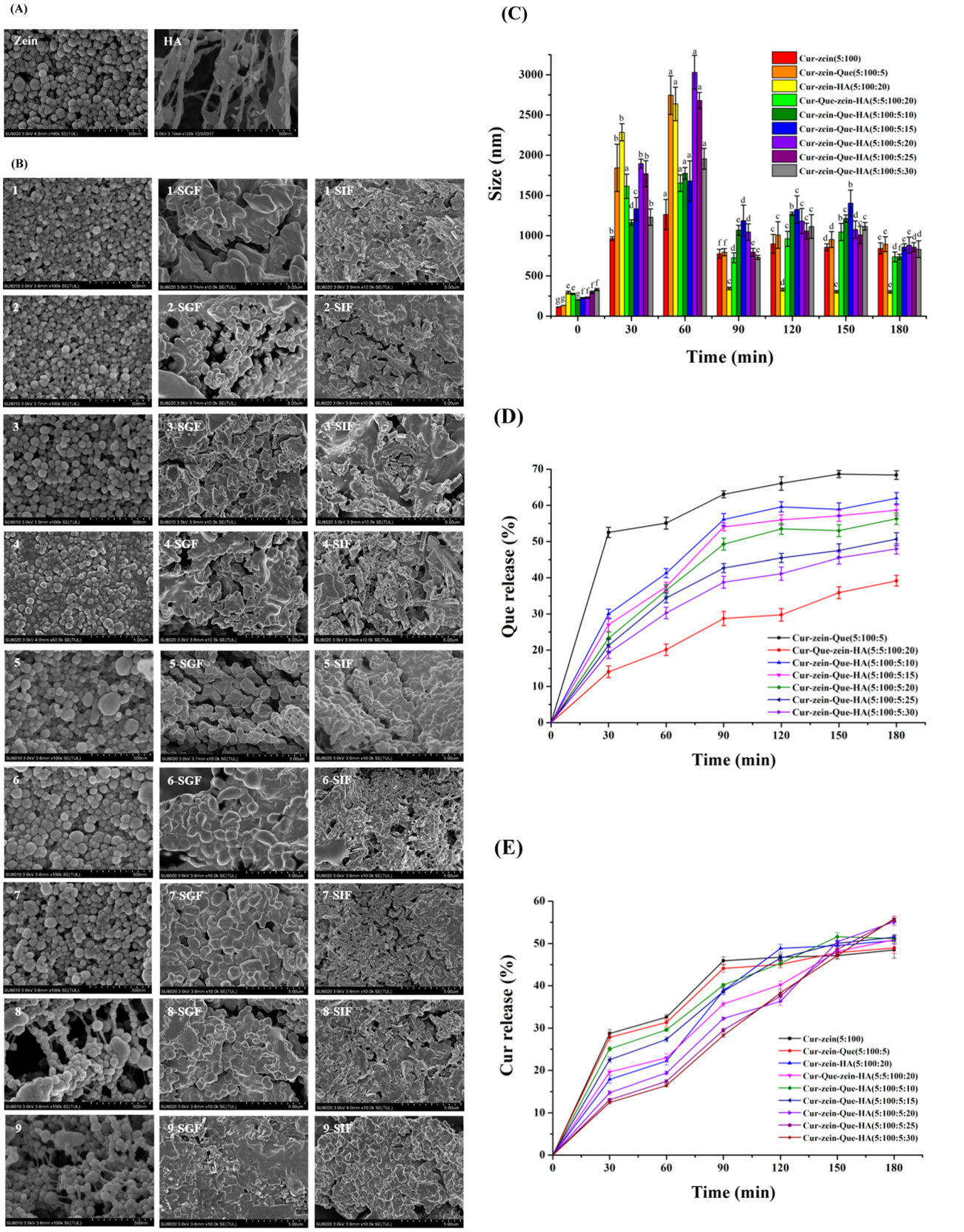

Figure 5. FE-SEM images of native zein and HA (A), and nanoparticles (B), (1–4) Cur–zein (5:100), Cur–zein–Que (5:100:5), Cur–zein–HA (5:100:20), and Cur–Que–zein–HA (5:5:100:20); (5–9) Cur–zein–Que–HA (5:100:5:10, 5:100:5:15, 5:100:5:20, 5:100:5:25, and 5:100:5:30) in simulated gastric fluids (SGF) and simulated intestinal fluids (SIF); mean size (C), quercetagetin release (D), and curcumin release (E) of Cur–zein–Que–HA nanoparticles in simulated gastrointestinal digestion.

DOI: 10.1021/acsami.9b02529
ACS Appl. Mater. Interfaces 2019, 11, 16922–16933

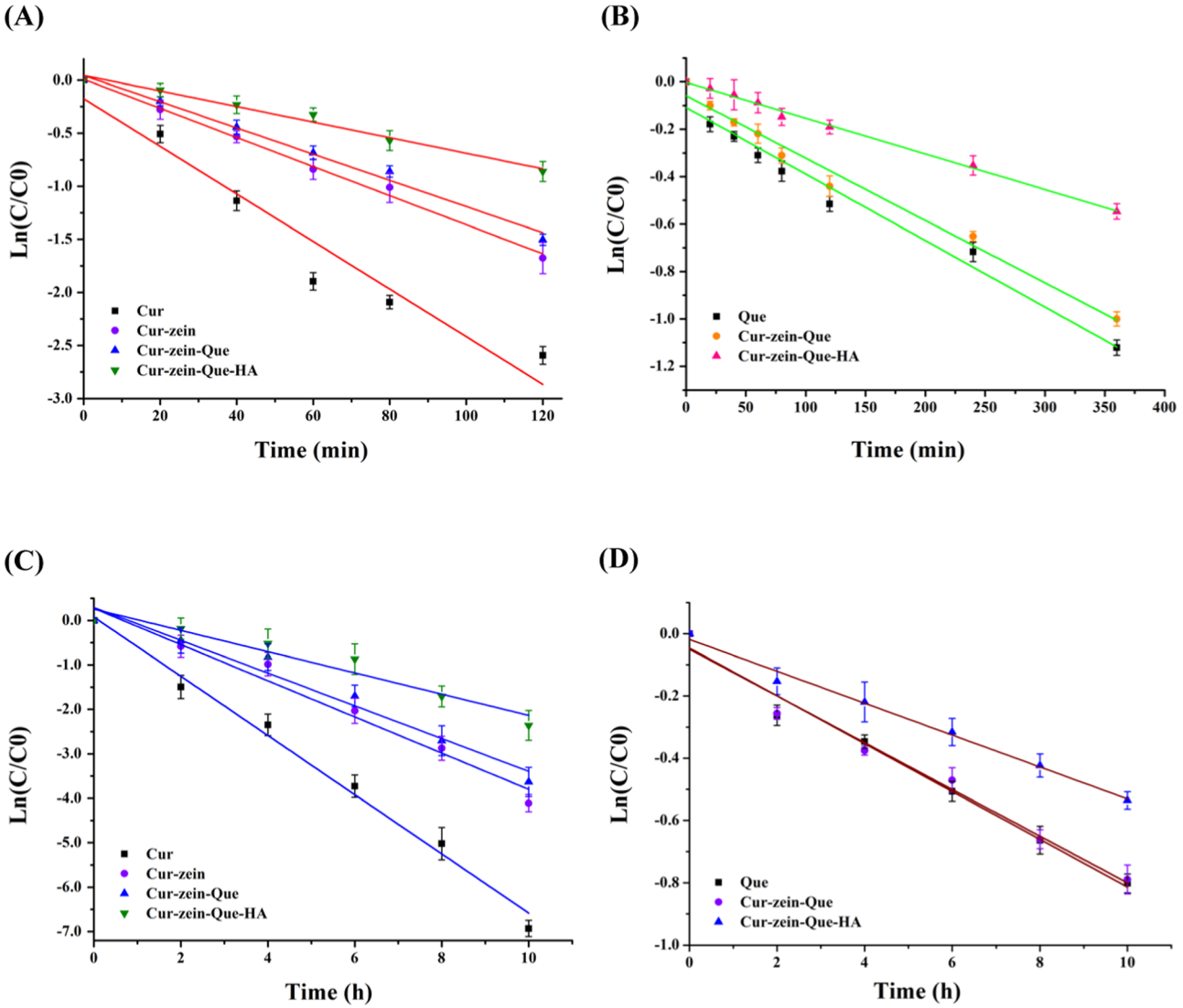

Figure 6. Light degradation kinetics (A, B) and thermal degradation kinetics (C, D) of curcumin and quercetagetin in Cur−zein−Que−HA nanoparticles.

5:100:5:10 to 5:100:5:30, the α-helix content increased, whereas the β-sheet content decreased.

3.6. Microstructure and Simulated Gastrointestinal Digestion. The microstructure of all of the samples was acquired using FE-SEM (Figure 5A,B). Native zein nanoparticles had a spherical shape,[41] whereas native HA exhibited a three-dimensional network structure (Figure 5A). The Cur−zein nanoparticles also had a spherical shape (Figure 5B), with a diameter larger than that of the zein nanoparticles, which suggests that the HA formed a coating. Cur−zein−Que (5:100:5), Cur−zein−HA (5:100:20), Cur−Que−zein−HA (5:5:100:20), and Cur−zein−Que−HA L-B-L nanoparticles (5:100:5:10, 5:100:5:15, and 5:100:5:20) were also spherical (Figure 5B). However, the Cur−zein−Que−HA nanoparticles (5:100:5:25 and 5:100:5:30) formed clusters. This structure may have been formed because HA promoted nanoparticle aggregation through a depletion or bridging mechanism or because the HA formed a microgel due to extensive hydrogen bonding among −OH, −COOH, and $-NHCOCH_3$ groups.[47] The HA microgel might then have trapped the zein nanoparticles inside.

After these samples were incubated within simulated gastric fluids (SGF), their microstructures were changed considerably (Figure 5B). After gastric digestion, Cur−zein (5:100) nanoparticles exhibited extensive aggregation, which may had occurred because pepsin and HCl hydrolyzed some of the zein molecules. Moreover, the particles were exposed to considerable changes in their pH and ionic strength, which will influence the electrostatic repulsion between them. Similarly, Zou et al.[48] also found that Cur−zein nanoparticles aggregate extensively in gastric digestion. After gastric digestion, Cur−zein−Que (5:100:5) nanoparticles also aggregated. When the nanoparticles were coated with a layer of HA, all of the samples tended to come together and form large clumps, particularly at higher HA levels. Other researchers have reported that HA can form aggregates under acidic conditions similar to those found in the gastric fluids.[49]

After digestion in simulated intestinal fluids (SIF), the microstructures of all of the samples indicated that they were highly aggregated, forming large clumps. This phenomenon is probably because the nanoparticles were partially digested by pancreatic enzymes (proteases) and were exposed to a change

DOI: 10.1021/acsami.9b02529
ACS Appl. Mater. Interfaces 2019, 11, 16922−16933

in solution conditions, such as ionic strength and pH, which altered the electrostatic interactions between them.[50]

The mean diameter of the nanoparticles increased substantially after digestion in the SGF (Figure 5C), but then decreased after digestion in the SIF. This effect can be attributed to particle aggregation in the gastric stage, followed by aggregate dissociation and disintegration in the intestinal stage, which is consistent with the FE-SEM images (Figure 5B). During gastrointestinal digestion, the nanoparticles were gradually broken down and the two nutraceuticals were released. Figure 5D shows that quercetagetin was released fairly rapidly from the Cur−zein−Que (5:100:5) nanoparticles during the first 30 min of digestion in the gastric stage. Subsequently, it was released more slowly, reaching a plateau value after about 90 min. These findings agreed with those of previous reports that have monitored the release of this nutraceutical under gastric conditions.[38] For the Cur−zein−Que−HA nanoparticles, quercetagetin was released more gradually throughout the simulated gastrointestinal conditions. As the HA concentration was increased, the release rate of quercetagetin decreased, which suggests that this may be an effective way to modulate the release profile of this nutraceutical in the human body. When quercetagetin was encapsulated in the Cur−Que−zein−HA (5:5:100:20) nanoparticles, its release rate was the slowest. This suggests that zein and HA had a synergistic effect on controlling its release.[38]

The curcumin release profile was also monitored under simulated gastrointestinal conditions (Figure 5E). Curcumin was released rapidly during 0−30 min and then more slowly during 30−60 min in the SGF stage. The release profiles were fairly similar for the Cur−zein and Cur−zein−Que nanoparticles, which suggests that quercetagetin did not interfere with curcumin release. During the first 90 min of digestion, the release of curcumin from the Cur−zein−Que−HA nanoparticles decreased as the HA level was increased, which suggests that the polymer coating was able to retard its release. After 150 min, however, the cumulative release of curcumin was fairly similar for all of the samples. These results revealed that the release rate of curcumin could be controlled by altering the design of the nanoparticles, but that the final extent is fairly similar for all systems.

3.7. Light and Thermal Degradation Kinetics. Nutraceuticals are often degraded during storage due to exposure to light or elevated temperatures. For this reason, the impact of light irradiation and heat treatment on the degradation kinetics of curcumin and quercetagetin in the nanoparticles were investigated (Figure 6). The half-life ($t_{1/2}$), rate constant (k), and correlation coefficient (R^2) calculated from the degradation curves are summarized in Tables S2 and S3. The half-life values indicated that both the light and thermal stabilities of curcumin increased in the following order: free Cur < Cur−zein < Cur−zein−Que < Cur−zein−Que−HA nanoparticles. The light stability of quercetagetin followed the same trend, free Que < Cur−zein−Que < Cur−zein−Que−HA nanoparticles, whereas its thermal stability was in the following order: free Que ≈ Cur−zein−Que < Cur−zein−Que−HA nanoparticles. Overall, these results show that encapsulation of the two nutraceuticals improved their light and thermal stabilities, with the effectiveness of protection depending on the particle design.

In terms of the light stability, the half-life of curcumin (30.9 min) was far lesser than that of quercetagetin (247.6 min). Similarly, in terms of thermal stability, the half-life of curcumin (1.04 h) was much lesser than that of quercetagetin (9.03 h). This result clearly indicates that curcumin is much less stable than quercetagetin under the conditions used.

In general, the Cur−zein−Que−HA nanoparticles were the most effective formulation for preventing both curcumin and quercetagetin from light and thermal degradation. This may have been because the chemically reactive groups in the C ring of the curcumin and quercetagetin were protected by being encapsulated in the nanoparticles through strong binding interactions.[18] Moreover, zein and HA may have been able to absorb some of the light waves that normally cause photodegradation, thereby protecting the nutraceuticals.

3.8. Long-Term Storage Stability. Finally, we investigated the stability of the Cur−zein−Que−HA nanoparticles during long-term storage so as to predict their potential shelf life in food products. These nanoparticle dispersions had a homogeneous cloudy yellow appearance (Figure S1), which can be ascribed to the presence of nanoparticles large enough to scatter light as well as to the selective light absorption by curcumin. The appearance of these samples did not change appreciably when they were stored for several months under refrigerated conditions, with no evidence of extensive color fading or sedimentation. As listed in Table S4, the mean sizes of the Cur−zein−Que−HA nanoparticles stored for 6 months were somewhat larger than those of the freshly prepared samples, which suggested that some aggregation had occurred. The result is in accord with a previous report that the diameter of zein−pectin−caseinate nanoparticles increased after 2 months of storage.[51] This observed increase in the particle diameter might be related to the reduction of charge on the nanoparticles during storage, which reduced the electrostatic repulsion between them. The absolute values of the ζ-potential of the nanoparticles decreased after 6 months of storage, which revealed that there was some change in their interfacial composition or structure.[52]

The retention of quercetagetin and curcumin in the nanoparticles was measured after 6 months of storage (Table S5). The retention of quercetagetin (31.8%) was slightly lower than that of curcumin (35.5%), which may have been because quercetagetin was located in the outer layer of the nanoparticles and therefore more exposed to the external environment. Conversely, curcumin was encapsulated into the hydrophobic core of the nanoparticles and therefore more protected from the surroundings.

When the nanoparticles were coated with HA, there was a reduction in quercetagetin and curcumin degradation. This protective effect increased as the level of HA within the nanoparticles increased. Based on our evaluation of the appearance, particle diameter, ζ-potential, and nutraceutical retention of the nanoparticles, it appears that they are a suitable delivery vehicle for both quercetagetin and curcumin.

4. CONCLUSIONS

In summary, a novel layer-by-layer composite nanoparticle has been fabricated that consists of a zein core and a HA shell. Curcumin was encapsulated inside the hydrophobic core of the zein nanoparticles, whereas quercetagetin was adsorbed onto their surfaces. The nanoparticles were then coated with a layer of HA molecules using electrostatic deposition. Both curcumin and quercetagetin were protected from photodegradation and thermal degradation by encapsulation, with the efficacy of the nanoparticles depending on their composition. For photodegradation, the half times of curcumin and quercetagetin in

DOI: 10.1021/acsami.9b02529
ACS Appl. Mater. Interfaces 2019, 11, 16922−16933

Cur−zein−Que−HA nanoparticles were 3- and 2-fold longer than those of free nutraceuticals, whereas for thermal degradation, they were 2.9-fold and 1.5-fold longer, respectively. Moreover, encapsulation of curcumin and quercetagetin was able to delay their release under simulated gastrointestinal conditions. We also showed that the optimized nanoparticles remained physically stable during storage, which is important for the development of commercial food products that utilize them. In conclusion, the nanoparticles developed in this study are a new form of codelivery system that might be useful for application in foods, supplements, and drugs. Nevertheless, further work is required to test their efficacy using animal and human studies.

■ ASSOCIATED CONTENT

Supporting Information

The Supporting Information is available free of charge on the ACS Publications website at DOI: 10.1021/acsami.9b02529.

Appearance of samples stored at 4 °C for 6 months; secondary structural content (%) of zein; light and thermal degradation kinetic parameters of curcumin and quercetagetin; particle size, ζ-potential, and retention rates of quercetagetin and curcumin of fresh and stored samples (PDF)

■ AUTHOR INFORMATION

Corresponding Author

*E-mail: gyxcau@126.com. Tel.: + 86-10-62737034. Fax: + 86-10-62737986.

ORCID

David Julian McClements: 0000-0002-9016-1291

Yanxiang Gao: 0000-0003-2331-5956

Notes

The authors declare no competing financial interest.

■ ACKNOWLEDGMENTS

Financial support from the National Natural Science Foundation of China (No. 31871842) is gratefully acknowledged. We are grateful for the Henan Key Laboratory of Cold Chain Food Quality and Safety Control (CCFQ2018-ZD-04) for funding. S.C. would like to thank the Chinese Scholarship Council for support. The characterization results were supported by Beijing Zhongkebaice Technology Service Co., Ltd.

■ REFERENCES

(1) Correa, S.; Dreaden, E. C.; Gu, L.; Hammond, P. T. Engineering Nanolayered Particles for Modular Drug Delivery. *J. Controlled Release* **2016**, *240*, 364−386.

(2) Oh, K. S.; Lee, H.; Kim, J. Y.; Koo, E. J.; Lee, E. H.; Park, J. H.; Kim, S. Y.; Kim, K.; Kwon, I. C.; Yuk, S. H. The Multilayer Nanoparticles Formed by Layer by Layer Approach for Cancer-Targeting Therapy. *J. Controlled Release* **2013**, *165*, 9−15.

(3) Pulakkat, S.; Balaji, S. A.; Rangarajan, A.; Raichur, A. M. Surface Engineered Protein Nanoparticles with Hyaluronic Acid Based Multilayers for Targeted Delivery of Anticancer Agents. *ACS Appl. Mater. Interfaces* **2016**, *8*, 23437−23449.

(4) Haidar, Z. S.; Hamdy, R. C.; Tabrizian, M. Protein Release Kinetics for Core-Shell Hybrid Nanoparticles Based on the Layer-by-Layer Assembly of Alginate and Chitosan on Liposomes. *Biomaterials* **2008**, *29*, 1207−1215.

(5) Luo, R.; Neu, B.; Venkatraman, S. S. Surface Functionalization of Nanoparticles to Control Cell Interactions and Drug Release. *Small* **2012**, *8*, 2585−2594.

(6) Shi, K.; Yu, H.; Lee, T. C.; Huang, Q. Improving Ice Nucleation Activity of Zein Film through Layer-By-Layer Deposition of Extracellular Ice Nucleators. *ACS Appl. Mater. Interfaces* **2013**, *5*, 10456−10464.

(7) Mei, L.; Teng, Z.; Zhu, G.; Liu, Y.; Zhang, F.; Zhang, J.; Li, Y.; Guan, Y.; Luo, Y.; Chen, X.; et al. Silver Nanocluster-Embedded Zein Films as Antimicrobial Coating Materials for Food Packaging. *ACS Appl. Mater. Interfaces* **2017**, *9*, 35297−35304.

(8) Lin, J.; Li, C.; Zhao, Y.; Hu, J.; Zhang, L. M. Co-Electrospun Nanofibrous Membranes of Collagen and Zein for Wound Healing. *ACS Appl. Mater. Interfaces* **2012**, *4*, 1050−1057.

(9) Jing, L.; Wang, X.; Liu, H.; Lu, Y.; Bian, J.; Sun, J.; Huang, D. Zein Increases the Cytoaffinity and Biodegradability of Scaffolds 3D-printed with Zein and Poly(E-Caprolactone) Composite Ink. *ACS Appl. Mater. Interfaces* **2018**, No. 18551.

(10) Chen, S.; Sun, C.; Wang, Y.; Han, Y.; Dai, L.; Abliz, A.; Gao, Y. Quercetagetin-Loaded Composite Nanoparticles Based on Zein and Hyaluronic Acid: Formation, Characterization, and Physicochemical Stability. *J. Agric. Food Chem.* **2018**, *66*, 7441−7450.

(11) Ganesh, S.; Iyer, A. K.; Morrissey, D. V.; Amiji, M. M. Hyaluronic Acid Based Self-Assembling Nanosystems for CD44 Target Mediated siRNA Delivery to Solid Tumors. *Biomaterials* **2013**, *34*, 3489−3502.

(12) Morton, S. W.; Poon, Z.; Hammond, P. T. The Architecture and Biological Performance of Drug-Loaded LbL Nanoparticles. *Biomaterials* **2013**, *34*, 5328−5335.

(13) Raia, N. R.; Partlow, B. P.; Mcgill, M.; Kimmerling, E. P.; Ghezzi, C. E.; Kaplan, D. L. Enzymatically Crosslinked Silk-Hyaluronic Acid Hydrogels. *Biomaterials* **2017**, *131*, 58−67.

(14) Dicker, K. T.; Gurski, L. A.; Pradhan-Bhatt, S.; Witt, R. L.; Farach-Carson, M. C.; Jia, X. Hyaluronan: A Simple Polysaccharide with Diverse Biological Functions. *Acta Biomater.* **2014**, *10*, 1558−1570.

(15) Silva, L. P. D.; Pirraco, R. P.; Santos, T. C.; Novoacarballal, R.; Cerqueira, M. T.; Rui, L. R.; Correlo, V. M.; Marques, A. P. Neovascularization Induced by the Hyaluronic Acid-Based Spongy-Like Hydrogels Degradation Products. *ACS Appl. Mater. Interfaces* **2016**, *8*, 33464−33474.

(16) Lee, W. H.; Loo, C. Y.; Young, P. M.; Traini, D.; Mason, R. S.; Rohanizadeh, R. Recent Advances in Curcumin Nanoformulation for Cancer Therapy. *Expert Opin. Drug Delivery* **2014**, *11*, 1183−201.

(17) Mehanny, M.; Hathout, R. M.; Geneidi, A. S.; Mansour, S. Exploring the Use of Nanocarrier Systems to Deliver the Magical Molecule; Curcumin and its Derivatives. *J. Controlled Release* **2016**, *225*, 1−30.

(18) Wang, W.; Liu, F.; Gao, Y. Quercetagetin Loaded in Soy Protein Isolate-κ-Carrageenan Complex: Fabrication Mechanism and Protective Effect. *Food Res. Int.* **2016**, *83*, 31−40.

(19) Ma, R. T.; Shi, Y. P. Magnetic Molecularly Imprinted Polymer for the Selective Extraction of Quercetagetin From Calendula Officinalis Extract. *Talanta* **2015**, *134*, 650−656.

(20) Baek, S.; Kang, N. J.; Popowicz, G. M.; Arciniega, M.; Jung, S. K.; Byun, S.; Song, N. R.; Heo, Y. S.; Kim, B. Y.; Lee, H. J.; et al. Structural and Functional Analysis of the Natural JNK1 Inhibitor Quercetagetin. *J. Mol. Biol.* **2013**, *425*, 411−423.

(21) Wang, Y.; Padua, G. W. Nanoscale Characterization of Zein Self-Assembly. *Langmuir* **2012**, *28*, 2429−2435.

(22) Wang, F.; Zhang, L.; Bai, X.; Cao, X.; Jiao, X.; Huang, Y.; Li, Y.; Qin, Y.; Wen, Y. Stimuli-Responsive Nanocarrier for Co-delivery of MiR-31 and Doxorubicin to Suppress High MtEF4 Cancer. *ACS Appl. Mater. Interfaces* **2018**, *10*, 22767−22775.

(23) Liu, F.; Ma, D.; Luo, X.; Zhang, Z.; He, L.; Gao, Y.; McClements, D. J. Fabrication and Characterization of Protein-phenolic Conjugate Nanoparticles for Co-delivery of Curcumin and Resveratrol. *Food Hydrocolloids* **2018**, *79*, 450−461.

(24) Yu, H.; Shi, K.; Liu, D.; Huang, Q. Development of a Food-Grade Organogel with High Bioaccessibility and Loading of Curcuminoids. *Food Chem.* **2012**, *131*, 48−54.
(25) Sun, C.; Dai, L.; Gao, Y. Binary Complex Based on Zein and Propylene Glycol Alginate for Delivery of Quercetagetin. *Biomacromolecules* **2016**, *17*, 3973−3985.
(26) Chen, S.; Xu, C.; Mao, L.; Liu, F.; Sun, C.; Dai, L.; Gao, Y. Fabrication and Characterization of Binary Composite Nanoparticles Between Zein and Shellac by Anti-Solvent Co-Precipitation. *Food Bioprod. Process.* **2018**, *107*, 88−96.
(27) Dai, L.; Li, R.; Wei, Y.; Sun, C.; Mao, L.; Gao, Y. Fabrication of Zein and Rhamnolipid Complex Nanoparticles to Enhance the Stability and in Vitro Release of Curcumin. *Food Hydrocolloids* **2018**, *77*, 617−628.
(28) Whitmore, L. The Peptaibol Database: A Database for Sequences and Structures of Naturally Occurring Peptaibols. *Nucleic Acids Res.* **2004**, *32*, D593−D594.
(29) Liu, Y.; Liu, D.; Li, Z.; Qian, G.; Le, X. Temperature-Dependent Structure Stability and in Vitro Release of Chitosan-Coated Curcumin Liposome. *Food Res. Int.* **2015**, *74*, 97−105.
(30) Mercali, G. D.; Gurak, P. D.; Schmitz, F.; Marczak, L. D. F. Evaluation of Non-Thermal Effects of Electricity On Anthocyanin Degradation During Ohmic Heating of Jaboticaba (Myrciaria Cauliflora) Juice. *Food Chem.* **2015**, *171*, 200−205.
(31) Patel, A.; Hu, Y.; Tiwari, J. K.; Velikov, K. P. Synthesis and Characterisation of Zein−Curcumin Colloidal Particles. *Soft Matter* **2010**, *6*, 6192−6199.
(32) Liang, H.; Zhou, B.; He, L.; An, Y.; Lin, L.; Li, Y.; Liu, S.; Chen, Y.; Li, B. Fabrication of Zein/Quaternized Chitosan Nanoparticles for the Encapsulation and Protection of Curcumin. *RSC Adv.* **2015**, *5*, 13891−13900.
(33) Peinado, I.; Lesmes, U.; Andres, A.; Mcclements, J. D. Fabrication and Morphological Characterization of Biopolymer Particles Formed by Electrostatic Complexation of Heat Treated Lactoferrin and Anionic Polysaccharides. *Langmuir* **2010**, *26*, 9827−9834.
(34) Bengoechea, C.; Jones, O. G.; Guerrero, A.; Mcclements, D. J. Formation and Characterization of Lactoferrin/Pectin Electrostatic Complexes: Impact of Composition, pH and Thermal Treatment. *Food Hydrocolloids* **2011**, *25*, 1227−1232.
(35) Sun, C.; Dai, L.; Gao, Y. Interaction and Formation Mechanism of Binary Complex Between Zein and Propylene Glycol Alginate. *Carbohydr. Polym.* **2017**, *157*, 1638−1649.
(36) Shinoda, K.; Carlsson, A.; Lindman, B. On the Importance of Hydroxyl Groups in the Polar Head-Group of Nonionic Surfactants and Membrane Lipids. *Adv. Colloid Interface Sci.* **1996**, *64*, 253−271.
(37) Li, J.; Shin, G. H.; Lee, I. W.; Chen, X.; Park, H. J. Soluble Starch Formulated Nanocomposite Increases Water Solubility and Stability of Curcumin. *Food Hydrocolloids* **2016**, *56*, 41−49.
(38) Sun, C.; Xu, C.; Mao, L.; Di, W.; Jie, Y.; Gao, Y. Preparation, Characterization and Stability of Curcumin-Loaded Zein-Shellac Composite Colloidal Particles. *Food Chem.* **2017**, *228*, 656−667.
(39) Yadav, D.; Kumar, N. Nanonization of Curcumin by Antisolvent Precipitation: Process Development, Characterization, Freeze Drying and Stability Performance. *Int. J. Pharm.* **2014**, *477*, 564−577.
(40) Cerqueira, M. A.; Souza, B. W. S.; Teixeira, J. A.; Vicente, A. A. Effect of Glycerol and Corn Oil on Physicochemical Properties of Polysaccharide Films-a Comparative Study. *Food Hydrocolloids* **2012**, *27*, 175−184.
(41) Liu, F.; Ma, C.; McClements, D. J.; Gao, Y. A Comparative Study of Covalent and Non-Covalent Interactions Between Zein and Polyphenols in Ethanol-Water Solution. *Food Hydrocolloids* **2017**, *63*, 625−634.
(42) Luo, Y.; Teng, Z.; Wang, Q. Development of Zein Nanoparticles Coated with Carboxymethyl Chitosan for Encapsulation and Controlled Release of Vitamin D3. *J. Agric. Food Chem.* **2012**, *60*, 836−843.
(43) Joye, I. J.; Davidov-Pardo, G.; Ludescher, R. D.; McClements, D. J. Fluorescence Quenching Study of Resveratrol Binding to Zein and Gliadin: Towards a More Rational Approach to Resveratrol Encapsulation Using Water-Insoluble Proteins. *Food Chem.* **2015**, *185*, 261−267.
(44) Souza, H. K.; Gonçalves, M. D. P.; Gómez, J. Effect of Chitosan Degradation On its Interaction with B-Lactoglobulin. *Biomacromolecules* **2011**, *12*, 1015−1023.
(45) Selling, G. W.; Hamaker, S. A.; Sessa, D. J. Effect of Solvent and Temperature on Secondary and Tertiary Structure of Zein by Circular Dichroism. *Cereal Chem.* **2007**, *84*, 265−270.
(46) Sun, C.; Yang, J.; Liu, F.; Yang, W.; Yuan, F.; Gao, Y. Effects of Dynamic High-Pressure Microfluidization Treatment and the Presence of Quercetagetin on the Physical, Structural, Thermal, and Morphological Characteristics of Zein Nanoparticles. *Food Bioprocess Technol.* **2016**, *9*, 320−330.
(47) Luan, T.; Wu, L.; Zhang, H.; Wang, Y. A Study On the Nature of Intermolecular Links in the Cryotropic Weak Gels of Hyaluronan. *Carbohydr. Polym.* **2012**, *87*, 2076−2085.
(48) Zou, L.; Zheng, B.; Zhang, R.; Zhang, Z.; Liu, W.; Liu, C.; Xiao, H.; McClements, D. J. Enhancing the Bioaccessibility of Hydrophobic Bioactive Agents Using Mixed Colloidal Dispersions: Curcumin-Loaded Zein Nanoparticles Plus Digestible Lipid Nanoparticles. *Food Res. Int.* **2016**, *81*, 74−82.
(49) Wu, S.; Ai, L.; Chen, J.; Kang, J.; Cui, S. W. Study of the Mechanism of Formation of Hyaluronan Putty at pH 2.5: Part I. Experimental Measurements. *Carbohydr. Polym.* **2013**, *98*, 1677−1682.
(50) Parris, N.; Cooke, P. H.; Hicks, K. B. Encapsulation of Essential Oils in Zein Nanospherical Particles. *J. Agric. Food Chem.* **2005**, *53*, 4788−4792.
(51) Veneranda, M.; Hu, Q.; Wang, T.; Luo, Y.; Castro, K.; Madariaga, J. M. Formation and Characterization of Zein-Caseinate-Pectin Complex Nanoparticles for Encapsulation of Eugenol. *LWT–Food Sci. Technol.* **2018**, *89*, 596−603.
(52) Wang, L.; Zhang, Y. Eugenol Nanoemulsion Stabilized with Zein and Sodium Caseinate by Self-Assembly. *J. Agric. Food Chem.* **2017**, *65*, 2990−2998.

DOI: 10.1021/acsami.9b02529
ACS Appl. Mater. Interfaces 2019, 11, 16922−16933